

Mechanochemical Synthesis of Chemically Stable Isoreticular Covalent Organic Frameworks

Bishnu P. Biswal,^{†,§} Suman Chandra,^{†,§} Sharath Kandambeth,^{†,§} Binit Lukose,[‡] Thomas Heine,[‡] and Rahul Banerjee^{*†}

[†]Physical and Materials Chemistry Division, CSIR-National Chemical Laboratory, Dr. Homi Bhabha Road, Pune 411008, India

[‡]Center for Functional Nanomaterials, School of Engineering and Science, Jacobs University Bremen, Research III, Room 61, Campus Ring 1, 28759 Bremen, Germany

S Supporting Information

ABSTRACT: Three thermally and chemically stable iso-reticular covalent organic frameworks (COFs) were synthesized via room-temperature solvent-free mechanochemical grinding. These COFs were successfully compared with their solvothermally synthesized counterparts in all aspects. These solvent-free mechanochemically synthesized COFs have moderate crystallinity with remarkable stability in boiling water, acid (9 N HCl), and base [TpBD (MC) in 3 N NaOH and TpPa-2 (MC) in 9 N NaOH]. Exfoliation of COF layers was simultaneously observed with COF formation during mechanochemical synthesis. The structures thus obtained seemed to have a graphene-like layered morphology (exfoliated layers), unlike the parent COFs synthesized solvothermally.

Construction of bonds through the simple, economical, and environmentally friendly mechanochemical (MC) route is of considerable interest in modern synthetic chemistry.¹ Recently mechanochemistry has been efficiently employed to carry out various organic and inorganic transformations, nanostructure formation, construction of metal–organic frameworks and thus has become a good alternative to classical solution-based synthesis.² A modified MC method was employed for the rapid synthesis of MOFs by using liquid-assisted grinding (LAG)^{2e} to enhance the topological selectivity and was also used to construct zero-dimensional (0D) porous organic cages.^{2f} Although mechanochemistry is well-known as one of the most suitable synthetic tools for the formation of covalent bonds, especially imine (Schiff base) condensation,^{1fg} not even a single attempt to synthesize 2D or 3D covalent organic frameworks (COFs) by an MC synthetic strategy has previously been made. COFs are lightweight, crystalline, porous materials constructed exclusively via strong covalent bonds between selected light elements such as C, Si, B, N, and O.³ The fundamental requirement for COF crystallization is reversibility in covalent bond formation; therefore, achieving the same via MC synthesis is a daunting challenge.⁴ In general, harsh experimental conditions (e.g., reaction in a sealed pyrex tube, inert atmosphere, suitable solvents, longer time for crystallization, etc.) are required during COF synthesis to form well-ordered crystalline frameworks. Moreover, once formed, COFs require special care in regard to storage because of their

moisture instability.^{4a} Hence, an advanced synthetic method such as MC grinding and proper optimization of the reaction conditions must be explored to overcome these issues. We very recently reported two highly stable COFs (TpPa-1 and TpPa-2) that were synthesized by using modified Schiff base reactions, where the proton tautomerism gave the framework exceptional stability toward water, acid, and base.⁵ The outstanding chemical stability of TpPa-1 and TpPa-2 led us to attempt an alternative simple, solvent-free, rapid, and scalable room-temperature construction of COFs through mechanochemistry.

Here we demonstrate for the first time the rapid, solvent-free, room-temperature MC synthesis of these COFs [denoted as TpPa-1 (MC) and TpPa-2 (MC)] by manual grinding in a mortar and pestle. These products were initially identified by visual color change, FT-IR spectra, and comparison of the powder X-ray diffraction (PXRD) profiles with those of their counterparts obtained by a solvothermal (ST) approach. In addition, following the same solvent-free MC route, we synthesized a new crystalline iso-reticular COF, TpBD (MC). For comparison, we also crystallized TpBD by the ST method along with TpPa-1 and TpPa-2. TpBD was found to be porous and highly crystalline with remarkable stability in boiling water, acid (9 N HCl), and base (3 N NaOH). Although TpPa-1 (MC), TpPa-2 (MC), and TpBD (MC) have moderate crystallinity compared with their ST counterparts TpPa-1, TpPa-2, and TpBD, their thermal and chemical stabilities are almost identical under similar experimental conditions (see the detailed discussion below). Interestingly, the mechanochemically synthesized COFs have a graphene-like layered morphology (exfoliated layers), in contrast to the COFs synthesized solvothermally.

The solvent-free MC syntheses of TpPa-1 (MC), TpPa-2 (MC), and TpBD (MC) were carried out using Schiff base aldehyde–amine condensation reactions. In a typical synthesis 1,3,5-triformylphloroglucinol (Tp) (0.30 mmol) and either *p*-phenylenediamine (Pa-1) (for TpPa-1), 2,5-dimethyl-*p*-phenylenediamine (Pa-2) (for TpPa-2), or benzidine (BD) (for TpBD) (0.45 mmol) were placed in a mortar and ground using a pestle at room temperature; after 5 min, a light-yellow powder (a mixture of oligomers and starting materials) was obtained

Received: February 19, 2013

Published: March 25, 2013

[Figure 1; also see section S-2 in the Supporting Information (SI)]. Over the next 15 min, the color changed from yellow to

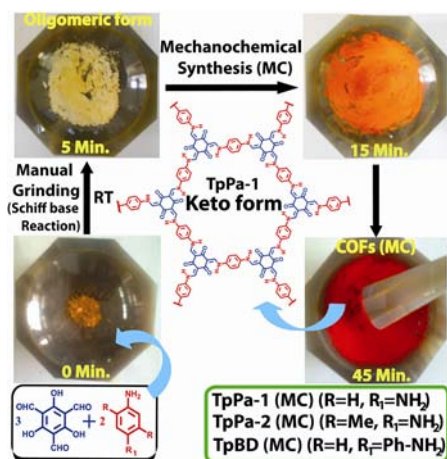


Figure 1. Schematic representation of the MC synthesis of **TpPa-1** (MC), **TpPa-2** (MC), and **TpBD** (MC) through simple Schiff base reactions performed via MC grinding using a mortar and pestle.

orange, perhaps as a result of an increase in the amount of conjugated units. Finally, after 40 min of grinding, a powdered material with a dark-red color (similar to that of the ST COFs) was obtained, indicating the complete COF formation. **TpBD** was also synthesized solvothermally by placing **Tp** (63 mg, 0.30 mmol), **BD** (82.9 mg, 0.45 mmol), 1:1 mesitylene/dioxane (3 mL), and 3 M aqueous acetic acid (0.5 mL) in a Pyrex tube for 72 h at 120 °C (section S-2).

PXRD was performed on **TpPa-1** (MC), **TpPa-2** (MC), and **TpBD** (MC) to ensure their crystallinity; they showed moderate crystallinity, exhibiting the first 2θ peak at low angles of 4.7, 4.7, and 3.3°, respectively, corresponding to the (100) reflection plane (Figure 2). The shift in 2θ from 4.7° to the lower value of 3.3° for **TpBD** (MC) could be due to isoreticulation, resulting in large pore apertures. In comparison with the solvothermally synthesized COFs, the first peak is relatively less intense for the mechanochemically synthesized COFs. This could be due to random displacement of the 2D layers (i.e., exfoliation), which may hinder the pore accessibility and hence affect the distributions of eclipsed pores. As a result, the reflection corresponding to the (100) plane becomes weak. The broad peak at higher 2θ ($\sim 27^\circ$) is mainly due to the π - π stacking between the COF layers and corresponds to the (001) plane. The d spacings for these three COFs were found to be

~ 3.4 , ~ 3.6 , and ~ 3.5 Å respectively. Proposed 2D models and detailed structural descriptions of **TpPa-1** and **-2** were presented in our previous publication.⁵ However, for **TpBD**, two possible 2D models (eclipsed and staggered) were built using the self-consistent charge–density functional tight-binding (SCC–DFTB) method, from which the unit cell parameters were calculated.⁶ All of the observed PXRD patterns for MC COFs matched well those of the ST COFs as well as the simulated patterns obtained using the eclipsed stacking model (Figure 2). For **TpBD**, the proposed model crystallizes in the hexagonal $P6/m$ space group with unit cell parameters $a = b = 29.287$ Å and $c = 3.250$ Å as derived from the Pawley refinements (section S-3).

To gain better insight to the bond formation and local mode of binding in the COFs synthesized mechanochemically, we investigated the progress of the reaction using FT-IR spectroscopy and compared the results with those for the COFs synthesized solvothermally (Figure 3a and section S-4). The three COFs synthesized mechanochemically showed FT-IR spectra similar to those of their solvothermally synthesized counterparts. The spectra obtained for all of these COFs clearly show the complete disappearance of the characteristic N–H stretching band of the free diamine (3100–3300 cm^{-1}), indicating complete consumption of the diamine. Simultaneously, the carbonyl (C=O) peak (at 1609 cm^{-1} , compared with 1639 cm^{-1} for **Tp**) broadens, shifts, and merges with the peak for the newly formed C=C bond (1582 cm^{-1}), which occurs because of the existence of strong hydrogen bonding in the keto form of the honeycomb 2D framework and confirms the *s-cis* structure. The absence of hydroxyl (O–H) and C=N stretching peaks and the appearance of the new C=C peak at 1582 cm^{-1} during formation of the 2D extended framework provide convincing evidence for the existence of the keto form, although the enol form was expected. Tautomerism drives the reaction toward the keto form instead of enol form, as further supported by comparison with the IR spectra of the reference compound 2,4,6-tris[(phenylamino)methylene]cyclohexane-1,3,5-trione (section S-4 and Figure S4 in the SI).^{7a} Two peaks, the [C=C(Ar)] peak at 1445 cm^{-1} and the C–N peak at 1256 cm^{-1} , are due to the aromatic C=C and newly formed C–N bonds in the keto form of the COF structure. The extra peak observed at 2885 cm^{-1} (C–H) for **TpPa-2** (MC) confirms the existence of the methyl group. In Figure 3a, the FT-IR profile of **TpPa-1** (MC) shows how the peak position changes with time during grinding, indicating the new bond formation and subsequently the construction of the COF network. We used ^{13}C cross-polarization magic-angle-spinning

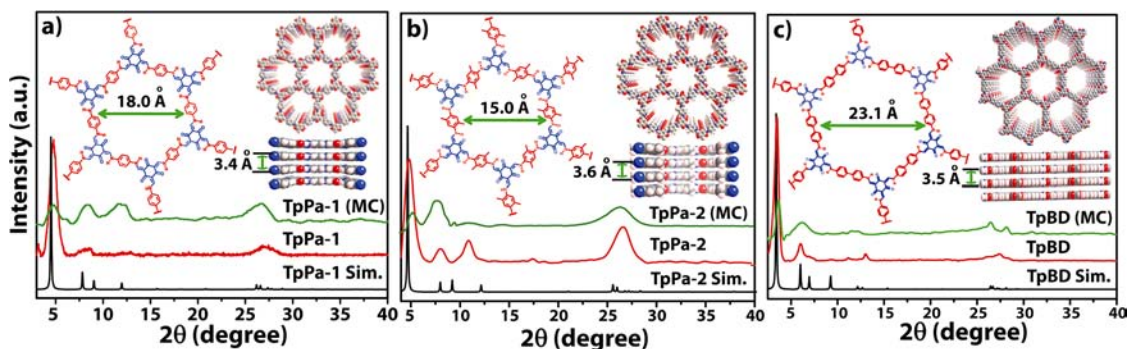


Figure 2. Comparison of the PXRD patterns for (a) **TpPa-1**, (b) **TpPa-2**, and (c) **TpBD**: (green) synthesized via MC grinding; (red) synthesized via the ST method; (black) simulated. The insets show the pore openings and π - π stacking distances between consecutive 2D layers.

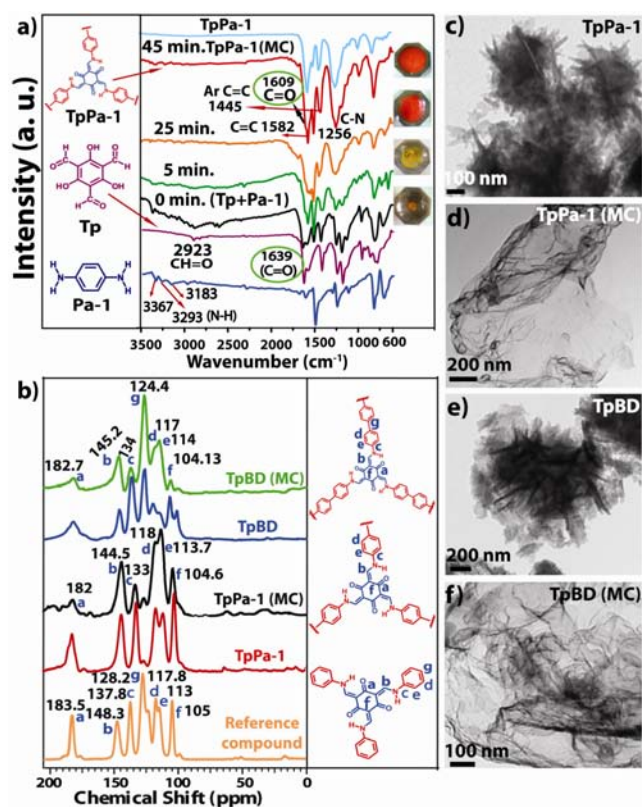


Figure 3. (a) Stepwise comparison of the FT-IR spectra showing the progress of the reaction with time for TpPa-1 (MC). Blue, brown, and black represent Pa-1, Tp, and the physical mixture of Tp and Pa-1, respectively, while green, golden yellow, and red represent the mixture after 5, 25, and 45 min of grinding, respectively. Cyan represents TpPa-1 synthesized by the ST method. The inset images at the right show the changes in color observed during grinding. (b) Comparison of the ¹³C CP-MAS solid-state NMR spectra of TpPa-1 (MC) (black), TpBD (MC) (green), TpPa-1 (red), TpBD (blue), and the reference compound 2,4,6-tris[(phenylamino)methylene]cyclohexane-1,3,5-trione (golden yellow). (c–f) High-resolution TEM images of TpPa-1, TpPa-1 (MC), TpBD, and TpBD (MC), respectively.

(CP-MAS) solid-state NMR spectroscopy to analyze the structural compositions of the COFs synthesized via MC grinding. The spectra obtained for the MC COFs were compared with those of the solvothermally synthesized COFs and the reference compound 2,4,6-tris[(phenylamino)methylene]cyclohexane-1,3,5-trione (Figure 3b). The exact match of the solid-state NMR profiles indicates that the COFs obtained by the two methods have the same local structure. All of the COFs show a signal at ~180 ppm that corresponds to the carbonyl carbon of the keto form. The absence of a peak at ~190 ppm gives clear evidence for the unavailability of the Tp starting material (section S-5). A peak appears at 124 ppm for the two identical carbons present at the biphenyl junction of TpBD (MC); this peak is absent for TpPa-1 (MC) and TpPa-2 (MC). For TpPa-2 (MC) there is a peak at 14 ppm due to the presence of extra methyl group, which is absent in TpPa-1 (MC) and TpBD (MC) (section S-5).

Scanning electron microscopy images indicated that small layers agglomerate to construct spherical-shaped particles with relative sizes of 5–7 μm for TpPa-1 (MC) and TpPa-2 (MC) (section S-8). However, for TpBD (MC), a flowerlike morphology was observed, as found previously for TpPa-1

and -2.⁵ Moreover, for TpBD (MC), these flower petals are exfoliated and well-dispersed with a graphene-sheet-like morphology. We observed this graphene-sheet-like layered morphology throughout the transmission electron microscopy (TEM) grid for TpPa-1 (MC), TpPa-2 (MC), and TpBD (MC) (Figure 3d,f and section S-9). These observations clearly show that the strong MC force applied to the already formed MC COFs causes exfoliation of the 2D layers, resulting in sheet-like structures. This kind of MC exfoliation is already known for graphene and other 2D materials, but the phenomenon presented here is the first to be observed for COF materials.^{7b,c}

Thermogravimetric analysis (TGA) profiles indicated that all of the COFs (MC and ST) have guest-free pores and thus have almost identical thermal stabilities up to ~350 °C (section S-7). However, framework decomposition occurs above 350 °C with a gradual weight loss of 45–60% for all of the COFs except TpBD (MC), where only 28% weight loss occurs up to 800 °C. Nitrogen adsorption–desorption experiments were performed to examine the architectural rigidity and permanent porosity of the MC and ST COFs at 77 K (Figure 4a). All of the COFs

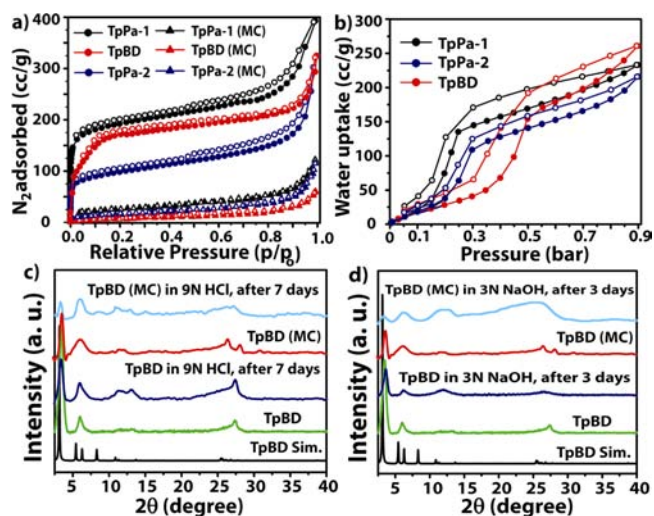


Figure 4. (a) Comparison of N₂ adsorption isotherms of TpPa-1 (MC), TpPa-2 (MC), and TpBD (MC) with those of TpPa-1, TpPa-2, and TpBD: black, blue, and red for TpPa-1, TpPa-2, and TpBD, respectively; solid and open symbols for adsorption and desorption, respectively; circles and triangles for ST and MC COFs, respectively. (b) Water adsorption isotherms for ST COFs at $P/P_0 = 0.9$ and 293 K. (c) Acid and (d) base stability tests for TpBD and TpBD (MC).

were solvent-exchanged (acetone/dichloromethane) and activated at 170 °C for 12 h under high-vacuum conditions prior to analysis to make the pores guest-free. They showed typical type-I reversible isotherms. The Brunauer–Emmett–Teller (BET) surface area for the newly introduced COF TpBD synthesized solvothermally was found to be 537 m²/g (values of 535 m²/g for TpPa-1 and 339 m²/g for TpPa-2 were reported previously). The COFs synthesized mechanochemically had lower BET surface areas of 61 m²/g for TpPa-1 (MC), 56 m²/g for TpPa-2 (MC), and 35 m²/g for TpBD (MC) (Figure 4a). The smaller surface area of TpBD (MC) compared with TpPa-1 (MC) could be due to its mesoporous nature, as the pore size distribution for TpBD was found to be 1.0–1.7 nm, calculated on the basis of nonlocal density functional theory (NLDFT) (section S-6 and Figure S10d in

the SI). The exact reason for the low surface areas for the MC COFs is not fully clear to us. However, we speculate that because of the MC exfoliation, which results in thin layered structures (Figure 3d,f), long-range pore formation in the MC COFs is hindered, and only less deep pores are accessible for N₂ sorption. Another possible reason could be the entrapment of oligomeric impurities inside the pores during the COF formation via MC grinding, although from the TGA profile we could not find any such contents. The H₂ uptake capacity of solvothermally synthesized **TpBD** was checked and found to be 0.7 wt % at 77 K, which is lower than those of **TpPa-1** (1.1 wt %) and **TpPa-2** (0.89 wt %).⁵ The CO₂ uptake of **TpBD** was 43 cm³/g at 273 K, compared with 78 cm³/g for **TpPa-1** and 64 cm³/g for **TpPa-2** at 273 K. We collected water vapor adsorption isotherms for all of the COFs (MC and ST) and found that **TpBD** has highest water vapor uptake [268 cm³/g at P/P₀ = 0.9 and 293 K], followed by **TpPa-1** (249 cm³/g) and **TpPa-2** (223 cm³/g) (Figure 4b and section S-6).

To investigate the stability of the MC- and ST-synthesized COFs in boiling water, we submerged 50 mg of COF in 10 mL of boiling deionized water (100 °C) for 7 days. After the mentioned period, PXRD data confirmed the crystallinity, as all of the PXRD peak positions and intensities remained intact (see section S-10 for all of the stability tests). Hence, we conclude that all of these COFs are highly stable in water. As explained in our recent paper, the water stability arises from the irreversible nature of the enol-to-keto tautomerism. The high stability of the MC COFs in water motivated us to check their stabilities toward acid and base. We previously observed the acid (9 N HCl) stability of **TpPa-1** and **TpPa-2** for 7 days time; hence, we also monitored the acid stability of all three MC COFs and the newly made **TpBD** in 9 N HCl for 7 days (Figure 4c). These COFs are highly stable in acid as well, as confirmed by the retention of the peak positions in the PXRD profiles collected after 7 days of treatment in 9 N HCl. We believe that the same phenomenon of tautomerism (forming only C–N bonds) plays a very crucial role in the exceptional acid stability of these COFs as well. **TpBD** and **TpBD** (MC) were stable in 3 N NaOH for ~3 days (Figure 4d), compared with **TpPa-1**, which is not stable in base for even 1 day, and **TpPa-2** (MC), which is stable for 7 days.

In summary, we for the first time have introduced a simple, solvent-free, room-temperature mechanochemical synthetic route for the construction of three chemically stable covalent organic frameworks [**TpPa-1** (MC), **TpPa-2** (MC), and **TpBD** (MC)]. Simple Schiff base mechanochemistry has been employed to synthesize these stable MC COFs efficiently at a higher rate and in high yield at room temperature. We have synthesized the new isorecticular COF **TpBD** (MC) using mechanochemistry and also crystallized the same COF via a solvothermal method. All of the MC COFs were found to be remarkably stable in boiling water, acid (9 N HCl), and base (3 N NaOH). MC exfoliation of 2D COF layers was observed during the grinding process, which has not been reported previously for COF materials. Although the crystallinity and porosity of these mechanochemically synthesized COFs are moderate, we believe that our strategy will provide better insight toward the synthetic development of stable COF materials and will eventually become a mainstream synthetic tool for large-scale COF production in the near future.

■ ASSOCIATED CONTENT

📄 Supporting Information

Synthetic procedures; PXRD, FT-IR, ¹³C solid-state NMR, and TGA data; and crystallographic data (CIF). This material is available free of charge via the Internet at <http://pubs.acs.org>.

■ AUTHOR INFORMATION

Corresponding Author

r.banerjee@ncl.res.in

Author Contributions

[§]B.P.B., S.C., and S.K. contributed equally.

Notes

The authors declare no competing financial interest.

■ ACKNOWLEDGMENTS

B.P.B. and S.C. acknowledge UGC and S.K. acknowledges CSIR for JRF. R.B. acknowledges CSIR (CSC0122) for funding. Financial assistance from DST (SR/S1/IC-22/2009) and BRNS (2011/37C/44/BRNS) is acknowledged.

■ REFERENCES

- (1) (a) MacGillivray, L. R.; Reid, J. L.; Ripmeester, J. A. *J. Am. Chem. Soc.* **2000**, *122*, 7817. (b) Morris, R. E.; James, S. L. *Angew. Chem., Int. Ed.* **2013**, *52*, 2163. (c) Aakeröy, C. B.; Sinha, A. S.; Epa, K. N.; Spartz, C. L.; Desper, J. *Chem. Commun.* **2012**, *48*, 11289. (d) James, S. L.; Adams, C. J.; Bolm, C.; Braga, D.; Collier, P.; Friščić, T.; Grepioni, F.; Harris, K. D. M.; Hyett, G.; Jones, W.; Krebs, A.; Mack, J.; Maini, L.; Orpen, A. G.; Parkin, I. P.; Shearouse, W. Ch.; Steed, J. W.; Waddell, D. C. *Chem. Soc. Rev.* **2012**, *41*, 413. (e) Tanaka, K.; Toda, F. *Chem. Rev.* **2000**, *100*, 1025. (f) Dolotko, O.; Wiench, J. W.; Dennis, K. W.; Pecharskya, V. K.; Balema, V. P. *New J. Chem.* **2010**, *34*, 25. (g) Rothenberg, G.; Downie, A. P.; Raston, C. L.; Scott, J. L. *J. Am. Chem. Soc.* **2001**, *123*, 8701.
- (2) (a) Friščić, T. *Chem. Soc. Rev.* **2012**, *41*, 3493. (b) Stojakovic, J.; Farris, B. S.; MacGillivray, L. R. *Chem. Commun.* **2012**, *48*, 7958. (c) Pichon, A.; Lazaun-Garay, A.; James, S. L. *CrystEngComm* **2006**, *8*, 211. (d) Friščić, T.; MacGillivray, L. R. *Chem. Commun.* **2003**, 1306. (e) Friščić, T.; Reid, D. G.; Halasz, I.; Stein, R. S.; Dinnebier, R. E.; Duer, M. J. *Angew. Chem., Int. Ed.* **2010**, *49*, 712. (f) Icli, B.; Christinat, N.; Tonnemann, J.; Schuttler, C.; Scopelliti, R.; Severin, K. *J. Am. Chem. Soc.* **2009**, *131*, 3154. (g) Orita, A.; Jiang, L.; Nakano, T.; Ma, N.; Otera, J. *Chem. Commun.* **2002**, 1362. (h) Friščić, T.; Halasz, I.; Beldon, P. J.; Belenguer, A. M.; Adams, F.; Kimber, S. A. J.; Honkimäki, V.; Dinnebier, R. E. *Nat. Chem.* **2013**, *5*, 66.
- (3) (a) Côté, A. P.; Benin, A. I.; Ockwig, N. W.; Matzger, A. J.; O’Keeffe, M.; Yaghi, O. M. *Science* **2005**, *310*, 1166. (b) Hienstmaier, J. F.; Medina, D. D.; Dogru, M.; Knochel, P.; Bein, T.; Dieck, W. M.; Lackinger, M. *ACS Nano* **2012**, *6*, 7234. (c) Colson, J. W.; Woll, A. R.; Mukherjee, A.; Levendorf, M. P.; Spittler, E. L.; Shields, V. B.; Spencer, M. G.; Park, J.; Dichtel, W. R. *Science* **2011**, *332*, 228.
- (4) (a) Lanni, L. M.; Tilford, R. W.; Bharathy, M.; Lavigne, J. J. *J. Am. Chem. Soc.* **2011**, *130*, 11872. (b) Furukawa, H.; Yaghi, O. M. *J. Am. Chem. Soc.* **2009**, *131*, 8875.
- (5) Kandambeth, S.; Mallick, A.; Lukose, B.; Mane, V. M.; Heine, T.; Banerjee, R. *J. Am. Chem. Soc.* **2012**, *134*, 19524.
- (6) (a) Heine, T.; Rapacioli, M.; Patchkovskii, S.; Frenzel, J.; Koester, A. M.; Calaminici, P.; Escalante, S.; Duarte, H. A.; Flores, R.; Geudtner, G.; Goursot, A.; Reveles, J. U.; Vela, A.; Salahub, D. R. *deMon-nano ed.*; 2009. (b) Lukose, B.; Kuc, A.; Heine, T. *Chem.—Eur. J.* **2011**, *17*, 2388.
- (7) (a) Chong, J. H.; Sauer, M.; Patrick, B. O.; MacLachlan, M. J. *Org. Lett.* **2003**, *5*, 3823. (b) Borriello, C.; De Maria, A.; Jovic, N.; Montone, A.; Schwarz, M.; Antisari, M. V. *Mater. Manuf. Processes* **2009**, *24*, 1053. (c) Jeon, I.-Y.; Choi, H.-J.; Jung, S.-M.; Seo, J.-M.; Kim, M.-J.; Dai, L.; Baek, J.-B. *J. Am. Chem. Soc.* **2013**, *135*, 1386.